



In-Cabin Radar Monitoring System: Detection and Localization of People Inside Vehicle Using Vital Sign Sensing Algorithm

A C Ramachandra, V Viswanatha, K Kishor, H Suhas and
E Pannir Selvam

EasyChair preprints are intended for rapid dissemination of research results and are integrated with the rest of EasyChair.

November 8, 2022

In-Cabin Radar Monitoring System: Detection and Localization of People Inside Vehicle using Vital Sign Sensing Algorithm

Ramachandra A C¹

Department of ECE

Nitte meenakshi Institute of technology
Bengaluru, India

Email- ramachandra.ac@nmit.ac.in

Viswanatha V²

Department of ECE

Nitte Meenakshi Institute of Technology
Bengaluru, India

Email – viswas779@gmail.com

Kishor K³

Department of ECE

Nitte Meenakshi Institute of Technology
Bengaluru, India

kishorreddy045@gmail.com

Suhas H⁴

Department of ECE

Nitte Meenakshi Institute of Technology
Bengaluru, India

suhasgowd006@gmail.com

Pannir Selvam E⁵

Department of RADAR

Veoneer India Pvt,Ltd
Bengaluru, India

pannir.selvam@gmail.com

Abstract— Radars are used in automobiles for various functionalities, starting from the obstacle alarm during vehicle reversing to advanced functionalities like autonomous driving. A practical method for monitoring people inside a vehicle for various applications (surveillance, safety, etc.) could be built using Radar. This paper presents the embedded implementation of a vital sign sensing algorithm using the radar signal processing (RSP) technique. MEX (MATLAB executable) interface is performed with the embedded C code of the vital sign sensing algorithm generated for validating the results with the RSP technique. Finally, Unit testing is performed on the developed embedded C code of the vital sign sensing algorithm to remove the dead codes and to verify whether all branches and statements in a developed algorithm are working accordingly. The embedded C code results were found to be matching precisely with the RSP technique. With the help of obtained results, we can differentiate between an adult and a baby inside a vehicle.

Keywords— CAN, Automotive, Embedded implementation, In-Cabin sensing, Lidar.

I. INTRODUCTION

Motor industry is the primary target of mmWave-0Wave radar applications [1]. Furthermore, there are also a number of different applications being studied in the business and healthcare sectors. For a number of therapeutic and diagnostic uses, such as disease diagnosis and oximetry, millimeter-0wave radars are being explored [2].

Human vital signs are tracked invisibly and remotely is one of the emerging application areas [3]. This is useful in a variety of situations, including going to monitor a large number of sleep seniors to accurately identify family conditions. In healthcare settings for toddlers and accident victims, in addition to use in driver observing to catch forgetfulness and fatigue in drivers to prevent accidents, the equipment is used for chronically sick patients if non-contact evaluations are preferred. Over last four decades, microwave remote scanning of physiological signals with proof of concepts for applications including sleep deprivation [5, 6], simultaneous infant and child mortality

syndrome (SIDS), and person identification using radar capture respiratory patterns [7], Doppler radar has been shown useful in application domains [4, 5].

In this paper, Embedded C code of vital sign algorithm is implemented for estimating the vital sign to differentiate between the Adult and a baby, using radar signal processing techniques. Furthermore, an MEX (MATLAB executable) interface is examined to validate the embedded C code, with the RSP algorithm developed in MATLAB as a reference. Finally, unit testing is performed for the developed embedded code.

II. THEORITICAL BACKGROUND

A. Signal Model

The basic premise of physiological radar is that a magnetic transmission is thrown at a human subject but also reflected off the adult's chest surface, causing phase shift [8-10]. The small

displacement of the chest surface related to cardio-respiratory activity is a direct function of phase shift of the reflected signal [11]-[13]. The frequency modulated transmitted signal is provided by the subsequent equation: [14]-[16]:

$$x_T(t) = A_T \cos(2\pi f_c t + \pi \frac{B}{T_c} t^2 + \phi(t)) \dots (1)$$

Where, the phase noise from the transmitter is given by $\phi(t)$

The indication of chirp beginning frequency is f_c

The chirp's bandwidth is represented by B

Every width of a chirp is expressed by T_c

Every period of chirp repetitions is specified by f_r

The outgoing signal is taken in by the radar in something like a scaled-down and time-shifted (by and t_d) form via:

$$x_R(t) = \alpha A_T \{ \cos(2\pi f_c(t - t_d) + \pi \frac{B}{T_c}(t - t_d)^2 + \phi(t - t_d)) \} \dots (2)$$

Where, time-delayed form of the reflected signal is called t_d .

$$t_d = \frac{2R(t)}{C} \dots (3)$$

$$\text{And } R(t) = r_0 + A_{br} \cos(2\pi f_{br}t) \dots (4)$$

Where,

$R(t)$ is the object radial range as shown in equation 4

Amplitude of the breathing rate is given by A_{br}

Breathing frequency is denoted by f_{br}

Speed of light is denoted by C

A further temporal shift (r) will happen in a radar with many receivers because of the relative distances between the different receiver components. Equation 5 displays the signal that each receiver element has received.

$$x_R(t)_i = \alpha A_i (\cos(2\pi f_c(t - t_d - ir) + \pi B f_r (t - t_d - ir)^2 + \phi(t - t_d - ir))) \dots (5)$$

$$\text{Where } r = \frac{d \sin \theta}{C}$$

i is the receiver element count, and θ is the angle of arrival. The transmitted phase and received phase from 1 and 2 are presented below, respectively.

$$A = 2\pi f_c t + \pi B f_r t^2 + \phi(t) \dots (6)$$

$$B_i = 2\pi f_c(t - t_d - ir) + \pi B f_r(t - t_d - ir)^2 + \phi(t - t_d - ir) \dots (7)$$

After I/Q mixing, the signal is provided below. The received signal is combined with a copy of the broadcast signal.

$$y_i(t) = A_r e^{j(A - B_i)} \dots (8)$$

Where, the received signal power is indicated by A_r

When a signal is received at the first antenna element, it is combined with a copy of the sent signal to create a single channel signal. This "In-phase" (I) signal is shown as follows simplification:

$$y(t) = A_r e^{j(2\pi f_c t + \pi B f_r t^2 + \phi(t) - 2\pi f_c(t - t_d) + \pi B f_r(t - t_d)^2 + \phi(t - t_d))} \dots (9)$$

On solving for the phase, we get

$$y(t) = A_r e^{j((-\frac{4\pi f_c A_{br}}{C} - \frac{4\pi f_r A_{br} t}{C}) \cos(2\pi f_{br}t) - \frac{4\pi f_c A_{br}}{C} - \frac{4\pi B f_r A_{br} t}{C})} \dots (10)$$

Concentrating on phase change in the slow time axis is adequate to extract breathing rate since the chest movement has a relatively modest amplitude (10 mm) and a low vibrational frequency (4 Hz) [8].

B. Advantages of Millimeter Wave Sensing

The sensitivity is substantially higher than microwave radar because the little move of the middle of the chest is in the millimeter scale and closely matches the radar wavelengths [9].

III. DESIGN AND METHODOLOGY

This portion of the article will focus on the implementation of vital sign algorithm in embedded C. Figure 1 shows the block diagram of vital sign estimation. The signal model is explained in Section 2. The phase extraction block extracts the phase information from the signal model. Once the phase extraction is done phase unwrapping is performed to obtain the actual displacement profile [18]-[19].

The DC or trend removal of the differential phase is carried out by computing ((t)-mean(t)) on every t . Then, the impulse-like noise is then removed by computing a forward (t - $t+1$) and backward (t - $t-1$) phase difference for each t . If these are greater than a defined standard, t is then replaced with a reconstructed value [20]-[21].

The breathing spectrum ranges between [0.1 – 0.5] Hz. By using the bandpass filter, we can limit the frequency values between those ranges.

FFT applied on the autocorrelated signal. The frequency corresponding to the maximum peak gives the corresponding breathing rate frequency. From this frequency, the

corresponding breathing rate is calculated in breaths per minute (bpm) [22]-[23].

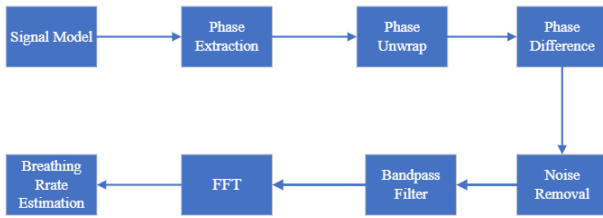


Figure 1 Block Diagram of Vital Sign Estimation

A. Embedded C implementation

Figure 2 shows the Embedded C code Implementation Flow Chart.

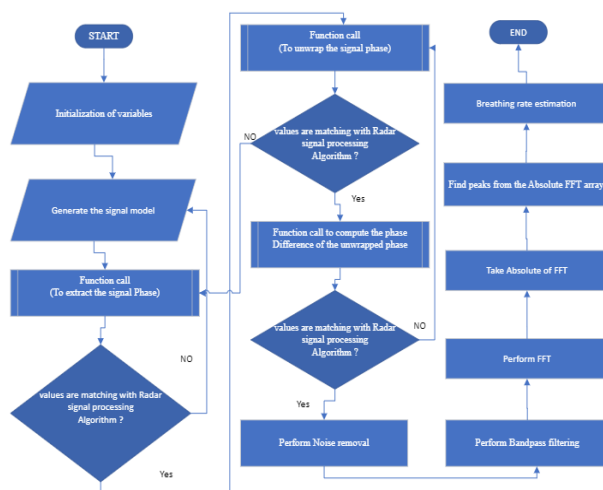


Figure 2 C code generation Flowchart

Above figure shows the flowchart for implementing an algorithm in Embedded C. Here main aim is to validate the results which we are implementing in Embedded C code, with the help of the Radar signal processing Algorithm. If results of Embedded C code are exactly matching with the Radar signal processing Algorithm, we can proceed the implementation otherwise we can correct it by travelling back to the previous step.

B. C Code and MEX Interface :Functional Implementation

This section deals with the interfacing the Embedded C Code with MATLAB Executable (MEX), MEX is an abbreviation for MATLAB Executable. We can use MATLAB to invoke custom C routines as if they were built-in functions thanks to MEX-files. Mex-files are referred to as M-functions in MATLAB. In this part, all code examples will be provided in C. the capability of immediately calling large-scale C or

FORTRAN functions from MATLAB without having to rewrite things as M-files. Users may recreate restrictive calculations, such for-loops, as a MEX-file to increase efficiency. Parallelism- For operations that can't be vectorized, you can develop multi-threaded C code.

Figure 3 shows the C MEX interface, where MATLAB (RSP algorithm) input is given to Embedded C logic. At the end both the RSP algorithm and Embedded C code produces the same output.

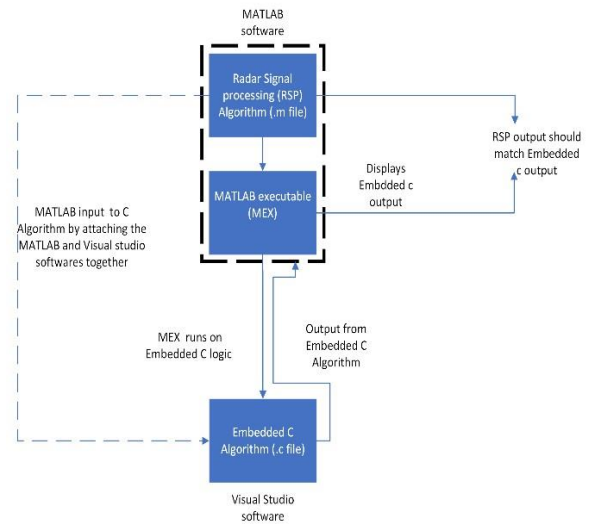


Figure 3 C MEX interface functional block diagram

IV. RESULTS AND DISCUSSION

In this section, we are discussing about the results obtained after validating the Embedded C code.

Before going to the results let us understand how respiratory rate varies across age [10]. Breathing information across Newborn to Adult is given in below table.

TABLE I. Acceptable Ranges for Respiratory Rates [14]

Acceptable Range OF Respiratorn Rates for Age	
Age	Rate (Breaths per Minuter)
New Born	30 – 40
Infant (6 Monts)	20 – 40
Toddler (2 years)	25 – 32
Child	20 – 30
Adolescent	16–19
Adult	12 – 20

By observing the above table, we can say that common breathing rate in adults are 12-20 BPM. Normal Breathing rate across the Newborn babies and children’s is 30 BPM.

Received phase: - figure 4 shown is the extracted phase from the original signal. This phase is obtained by performing arc tangent operation for the generated signal. By referring figure 4 we can say that both the RSP and Embedded C graph are matching each other.

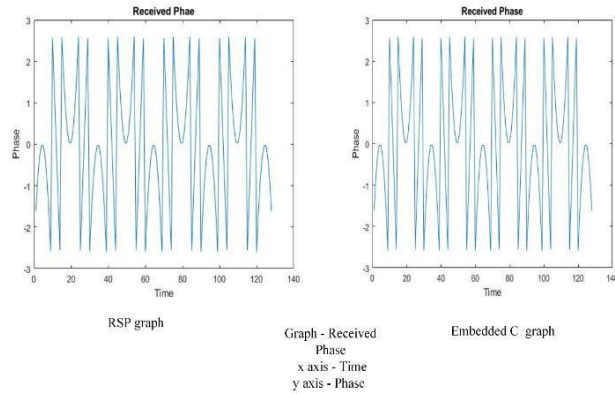


Figure 4 Received Phase for 20 BPM

Unwrapped Phase: - figure 5 shows the unwrapped phase, this unwrapped phase is obtained by performing unwrap operation on the received phase. This operation is performed to obtain the actual displacement profile. By referring figure 5 we can say that both the RSP and Embedded C graphs are matching each other.

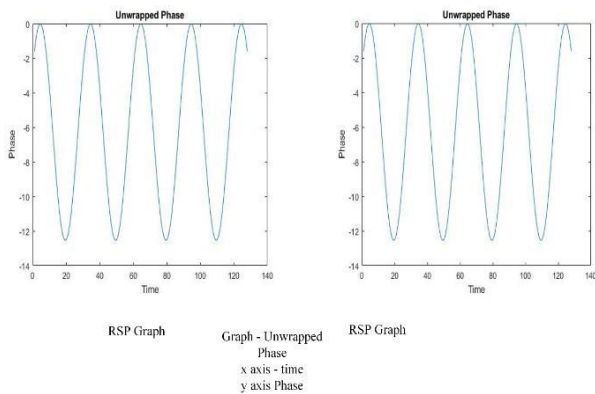


Figure 5 Unwrapped Phase for 20 BPM

Phase Difference: - Figure 6 shows the phase difference plot, which is extracted from the unwrapped phase. By performing phase difference operation for the unwrapped phase, we can obtain the phase-difference plot. By referring the RSP graph and Embedded C graph we can say that both the graphs are matching each other.

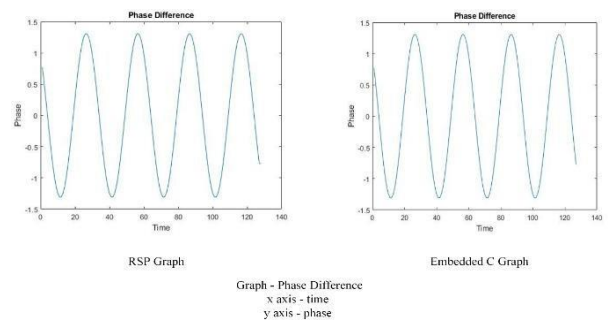


Figure 6 Phase difference for 20BPM

FFT and Peak picking: - FFT is performed. By looking into the peaks in the FFT spectrum we can estimate the breathing rate. FFT graph is shown in the figure 8. Figure 9 shows a peak picking from the FFT array.

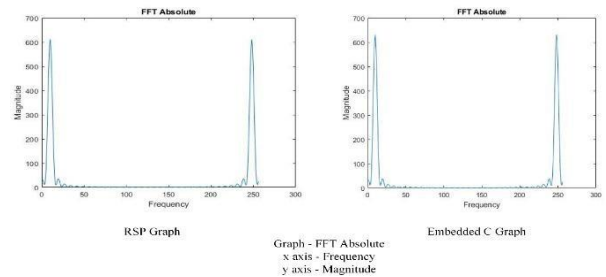


Figure 7 Absolute FFT

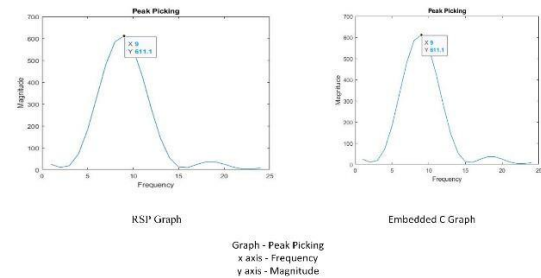


Figure 8 peak picking from FFT spectrum

V. CONCLUSION AND FUTURE SCOPE

In this project Embedded C code is implemented with the help of Radar signal Processing technique. Algorithm which is developed in embedded C is matching exactly with the Radar signal processing (RSP) Algorithm. we can differentiate between the adult and a baby by calculating the exact breaths per minute (BPM) value.

The developed embedded C code can estimate the respiration rate based on the chest displacement.

Future scope for the current project is defines below.

We can extend this technique for extraction of heart beat.

We can port the developed algorithm to the hardware, where this hardware board can be interfaced in a car for the purpose of breathing rate measurement, to differentiate between adult and a baby.

REFERENCES

- [1] S, R. D., L. . Shyamala, and S. . Saraswathi. "Adaptive Learning Based Whale Optimization and Convolutional Neural Network Algorithm for Distributed Denial of Service Attack Detection in Software Defined Network Environment". *International Journal on Recent and Innovation Trends in Computing and Communication*, vol. 10, no. 6, June 2022, pp. 80-93, doi:10.17762/ijritcc.v10i6.5557.
- [2] Boyapati, B. ., and J. . Kumar. "Parasitic Element Based Frequency Reconfigurable Antenna With Dual Wideband Characteristics for Wireless Applications". *International Journal on Recent and Innovation Trends in Computing and Communication*, vol. 10, no. 6, June 2022, pp. 10-23, doi:10.17762/ijritcc.v10i6.5619.
- [3] J. Hasch, E. Topak, R. Schnabel, T. Zwick, R. Weigel, and C. Waldschmidt, "Millimeter-wave technology for automotive radar sensors in the 77 ghz frequency band," *IEEE Transactions on Microwave Theory and Techniques*, vol. 60, no. 3, pp. 845–860, 2012.
- [4] F. Topfer and J. Oberhammer, "Millimeter-wave tissue diagnosis: The most promising fields for medical applications," *Microwave Magazine, IEEE*, vol. 16, no. 4, pp. 97–113, 2015.
- [5] Gupta, D. J. . (2022). A Study on Various Cloud Computing Technologies, Implementation Process, Categories and Application Use in Organisation. *International Journal on Future Revolution in Computer Science & Communication Engineering*, 8(1), 09–12. <https://doi.org/10.17762/ijfrcsce.v8i1.2064>
- [6] C. Gu, "Short-range noncontact sensors for healthcare and other emerging applications: A review," *Sensors (Basel, Switzerland)*, vol. 16, no. 8, p. 1169, 2016.
- [7] J. C. Lin, "Noninvasive microwave measurement of respiration", *Proc. IEEE*, vol. 63, no. 10, pp. 1530, Oct. 1975.
- [8] Meheran Baboli, Aditya Singh, Bruce Soll, Olga Boric-Lubecke and Victor Lubecke, "Good Night: Sleep Monitoring Using a Physiological Radar Monitoring System Integrated with a Polysomnography System", *IEEE Microwave Magazine*, vol. 16 (6), pp. 34-41, 2015.
- [9] Viswanatha, V., and R. Venkata Siva Reddy. "Research on state space modeling, stability analysis and PID/PIDN Control of DC–DC converter for digital implementation." *Advances in Electrical and Computer Technologies*. Springer, Singapore, 2020. 1255-1272.
- [10] Viswanatha, V. "Stability and Dynamic Response of Analog and Digital Control loops of Bidirectional buck-boost Converter for Renewable Energy Applications." *International Journal of Recent Technology and Engineering*, Volume-8 Issue-2, July 201 (2019).
- [11] Noah Hafner, Isar Mostafanezhad, Victor M. Lubecke, Olga BoricLubecke, and Anders Host-Madsen, "Non-contact Cardiopulmonary Sensing with a Baby Monitor", *Annual International Conference of the IEEE Engineering in Medicine and Biology Society (EMBC'07)*, pp. 2300-2302, 2007.
- [12] Shekh M Islam, Ashikur Rahman, Narayana Prasad, Olga BoricLubecke and Victor M. Lubecke, "Identity Authentication System using Support Vector Machine (SVM) on Radar Respiration Measurement", *93rd ARFTG Microwave Measurement Conference (ARFTG'19)*, pp. 1- 4, 2019.
- [13] Shekh M Islam, Ashikur Rahman, Narayana Prasad, Olga BoricLubecke and Victor M. Lubecke, "Identity Authentication System using Support Vector Machine (SVM) on Radar Respiration Measurement", *93rd ARFTG Microwave Measurement Conference (ARFTG'19)*, pp. 1- 4, 2019.
- [14] Andrie Dazlee, N. M. A., Abdul Khalil, S., Abdul-Rahman, S., & Mutalib, S. (2022). Object Detection for Autonomous Vehicles with Sensor-based Technology Using YOLO. *International Journal of Intelligent Systems and Applications in Engineering*, 10(1), 129–134. <https://doi.org/10.18201/ijisae.2022.276>
- [15] Viswanatha, V., and R. Reddy. "Characterization of analog and digital control loops for bidirectional buck–boost converter using PID/PIDN algorithms." *Journal of Electrical Systems and Information Technology* 7.1 (2020): 1-25.
- [16] Shekh M Islam, Ehsan Yavari, Ashikur Rahman, Olga Boric-Lubecke and Victor M. Lubecke, "Separation of Respiratory Signatures for Multiple Subjects using Independent Component Analysis with the JADE Algorithm", *40th IEEE Engineering in Medicine and Biology Society (EMBC'18)*, pp. 345-349, 2018.
- [17] Shekh M Islam, Ehsan Yavari, Ashikur Rahman, Olga Boric-Lubecke and Victor M. Lubecke, "Multiple Subject Respiratory Pattern Recognition and Estimation of direction of arrival using phasecomparison monopulse radar", *2019 IEEE Radio & Wireless Week (RWW'19)*, pp. 323-325, 2019.
- [18] N. A. Libre. (2021). A Discussion Platform for Enhancing Students Interaction in the Online Education. *Journal of Online Engineering Education*, 12(2), 07–12. Retrieved from <http://onlineengineeringeducation.com/index.php/joe/article/view/49>
- [19] Shekh M Islam, Ehsan Yavari, Ashikur Rahman, Olga Boric-Lubecke and Victor M. Lubecke, "Direction of Arrival Estimation of Physiological Signals for Multiple Subjects Using Phase Comparison Monopulse Radar", *2018 Asia-Pacific Microwave Conference (APMC'18)*, pp. 411-413, 2018.
- [20] Adeel Ahmad, June Chul Roh, Dan Wang, and Aish Dubey, "Vital Signs Monitoring of Multiple People Using a FMCW Millimeter-wave Sensor", *2018 IEEE Radar Conference*, pp. 1450-1455.

-
- [21] G. M. Brooker, "Understanding millimeter wave FMCW radars", 1st International Conference on Sensing Technology, Palmerston North, New Zeland, 2005.
- [22] Degambur, L.-N., Mungur, A., Armoogum, S., & Pudaruth, S. (2022). Resource Allocation in 4G and 5G Networks: A Review. *International Journal of Communication Networks and Information Security (IJCNIS)*, 13(3).
- [23] L. Oliveira, J. C. B. Mattos and L. Brisolaro, "Survey of Memory Optimization Techniques for Embedded Systems," 2013 III Brazilian Symposium on Computing Systems Engineering, 2013, pp. 65-70, doi: 10.1109/SBESC.2013.35.
- [24] V. Viswanatha and R. Venkata Siva Reddy, "Modeling, simulation and analysis of noninverting buck-boost converter using PSIM," 2016 International Conference on Circuits, Controls, Communications and Computing (I4C), 2016, pp. 1-5.
- [25] V. Viswanatha and R. V. S. Reddy, "Digital control of buck converter using arduino microcontroller for low power applications," 2017 International Conference on Smart Technologies for Smart Nation (SmartTechCon), 2017, pp. 439-443.
- [26] Rekha, V., M. Padmanabharaju, B. T. P. Madhav, and S. S. M. Reddy. "Triple Band Textile Array Antenna With Enhanced Gain and Low SAR for Off Body Communication Applications". *International Journal on Recent and Innovation Trends in Computing and Communication*, vol. 10, no. 6, June 2022, pp. 44-51, doi:10.17762/ijritcc.v10i6.5626.
- [27] J. P., and A. V. S. . Kumar. "A Scheme for Detecting the Sinkhole for Secured WSN". *International Journal on Recent and Innovation Trends in Computing and Communication*, vol. 10, no. 7, July 2022, pp. 28-37, doi:10.17762/ijritcc.v10i7.5562.